

Abstract

Tropospheric ozone (O_3) is a known greenhouse gas responsible for impacts on human and animal health and ecosystem functioning. In addition, O_3 plays an important role in tropospheric chemistry, together with nitrogen oxides. Flux measurements of these trace gases are a major issue to establish their atmospheric budget and evaluate the ozone impact onto the biosphere. In this study, ozone, nitric oxide (NO) and nitrogen dioxide (NO_2) fluxes were measured using the aerodynamic gradient method over a bare soil in an agricultural field. Vertical mixing ratio profile measurements were performed with fast response sensors. It was demonstrated that corrections of the aerodynamic gradient for chemical reactions between O_3 -NO- NO_2 appeared to be negligible for O_3 fluxes, whereas they accounted for about 10 % on average of the NO and NO_2 fluxes. The flux uncertainties were mainly due to uncertainties of the friction velocity. In addition, the use of fast response sensors allowed to reduce the remaining part of the flux uncertainty. The aerodynamic gradient and eddy-covariance methods gave similar O_3 fluxes (within 4 %). The chamber NO fluxes were up to 70 % lower than the aerodynamic gradient fluxes probably caused by either the spatial heterogeneity of the soil NO emissions or the environmental perturbation due to the chamber.

1 Introduction

Tropospheric ozone (O_3) is a common greenhouse gas responsible for a non negligible part of the radiative forcing (IPCC, 2007). In addition, O_3 is a major pollutant having impacts on human (and animal) health and ecosystem functioning (PORG, 1997; Paoletti, 2005; Paoletti and Grulke, 2005; Ainswoth, 2008; Wittig et al., 2009). Since the 1950s, background O_3 concentrations have doubled and the annual average ozone mixing ratio ranges from 20 to 45 ppb, depending on the geographical location (Vingarzan, 2004). The current global scale pollution models predict an increase in O_3 concentrations by a factor of 2–4 in the coming century (Vingarzan, 2004). Based on recent

AMTD

4, 5481–5527, 2011

Comparison of methods for the determination of NO - O_3 - NO_2 fluxes

P. Stella et al.

Title Page

Abstract

Introduction

Conclusions

References

Tables

Figures

◀

▶

◀

▶

Back

Close

Full Screen / Esc

Printer-friendly Version

Interactive Discussion

ecosystem modelling studies, which include O₃ impacts on plants, it is thought that this increase in O₃ would lead to a decrease in CO₂ absorption by terrestrial ecosystems, which would provide a positive feedback in the atmospheric greenhouse gas budget (Felzer et al., 2007; Sitch et al., 2008).

5 Nitrogen oxides (NO_x = NO + NO₂) are well known for their major role in tropospheric chemistry, in particular for their contribution to the photochemical formation of O₃ (Fowler et al., 1998, 1999), and thus their indirect contribution to global warming. Nitrogen oxides are released into the atmosphere from a variety of sources, the major being fossil fuel combustion, and biomass burning. However, soil microbial emissions
10 are also of high interest, especially as they are diffusive sources, which therefore affect the atmospheric chemistry over large areas (Delmas et al., 1997). Global NO_x emissions have increased from 12 Tg_{N-NO_x} yr⁻¹ during the pre-industrial area to 40–50 Tg_{N-NO_x} yr⁻¹ actually (Denman et al., 2007). Soil nitric oxide (NO) emissions from agricultural soils are estimated to represent 40 % of the total soil NO emission (Yienger and Levy, 1995; Aneja and Robarge, 1996). Soil nitric oxide emissions occur mainly through the nitrification and denitrification processes and depend on several factors. The main drivers are the amount of nitrogen fertilization, the soil temperature and soil moisture (Laville et al., 2009).

20 The extent to which terrestrial ecosystems intervene in the atmospheric budget of O₃ and NO_x is of high interest. Several studies have been performed to understand and evaluate the capacity of ecosystems to represent sources or sinks for O₃ (Lamaud et al., 2002, 2009; Zhang et al., 2002, 2006; Altimir et al., 2004, 2006; Gerosa et al., 2004; Rummel et al., 2007; Coyle et al., 2009) and NO_x (Butterbach-Bahl et al., 2002; Rummel et al., 2002; Fang and Mu, 2007; Li and Wang, 2007; Sanchez-Martin et al.,
25 2008; Laville et al., 2009, 2011).

Several methods are known to measure trace gas fluxes between the atmosphere and the biosphere. Among the numerous techniques used, it is possible to distinguish between the micrometeorological methods, such as the eddy-covariance (EC) (and those derived such as relaxed eddy-accumulation and disjunct eddy-covariance),

Comparison of methods for the determination of NO-O₃-NO₂ fluxes

P. Stella et al.

Title Page

Abstract

Introduction

Conclusions

References

Tables

Figures

⏪

⏩

◀

▶

Back

Close

Full Screen / Esc

Printer-friendly Version

Interactive Discussion



Comparison of methods for the determination of NO-O₃-NO₂ fluxes

P. Stella et al.

Title Page

Abstract

Introduction

Conclusions

References

Tables

Figures

⏪

⏩

◀

▶

Back

Close

Full Screen / Esc

Printer-friendly Version

Interactive Discussion



and the aerodynamic gradient methods (AGM) (Foken, 2008), or the chamber methods (Meixner et al., 1997; Denmead, 2008). The micrometeorological methods allow measurements at the landscape scale (from few hectares to several square kilometres), whereas chambers represent the smallest scale (around 1 m²). The eddy covariance method has been extensively used for studying carbon dioxide and water vapour exchanges in a network of flux measurement sites such as CarboEuroFlux (Aubinet et al., 2000), AmeriFlux (Running et al., 1999), Fluxnet (Baldocchi et al., 2001), CarboEurope-IP (Dolman et al., 2006) and NitroEurope-IP (Skiba et al., 2009) and became the reference method for flux measurements. Nevertheless, for trace gases for which there is a lack of fast response sensors, such as NH₃, the use of aerodynamic gradient methods is still a reference method (e.g. Milford et al., 2009). Moreover, the estimation of fluxes of chemically reactive species, especially ozone, nitric oxide and nitrogen dioxide, requires measuring both the concentrations and the fluxes at several heights to estimate the flux divergence due to chemical reactions (Kramm et al., 1991, 1995; Duyzer et al., 1995). Alternatively, one could measure the flux at several heights simultaneously with the EC method, but this would require several instruments. Nevertheless, there are only few studies reporting comparisons of measurement methods, especially for O₃ and NO_x, and some of them report contradictory results. As an example, Muller et al. (2009) found a large overestimation in ozone deposition with the AGM when compared to the EC method, whereas Keronen et al. (2003) reported similar values using these two methods. In addition, the few previous comparison studies did not correct the fluxes for chemical reactions before comparing the different methods.

This study reports measurements of NO-O₃-NO₂ fluxes over an agricultural field after wheat harvest, tillage and slurry incorporation. The aim of this study was to measure NO-O₃-NO₂ fluxes by the AGM with a profile system, composed only of fast response sensors. A strong emphasis was given to the quality and uncertainty estimation of the fluxes, as well as on the impact of chemistry between NO_x and O₃ on the flux divergences. The results of the AGM are compared with O₃ fluxes measured by

eddy-covariance and with NO fluxes measured using automatic chambers. Finally, the measured fluxes are discussed and compared to previous studies.

2 Materials and methods

2.1 Site description and meteorological measurements

5 The experimental site is an agricultural field located at Grignon (48°51' N, 1°58' E), 40 km west of Paris. The size of the field is 19 ha with a winter wheat-maize-winter barley-mustard rotation. The soil is a silt loam (31 % clay, 62.5 % silt and 6.5 % sand). The site is surrounded by quite heavy traffic roads on the east, south and south-west, with peaks of traffic between 06:00–07:00 UT and 20:00–22:00 UT. The site is in the
10 plume of Paris during east-north-easterly winds, while the air is relatively clean during south-westerly to north-westerly winds. More details of the site can be found in Laville et al. (2009, 2011), and Loubet et al. (2011).

The experiment was carried out from 20 to 30 August 2009, following cattle slurry incorporation of 98.5 kg_{N-NH₄} ha⁻¹ and tillage at 5 cm depth on 5 August 2009. Wheat
15 was harvested just before 31 July 2009. The surface was therefore a mix of bare soil and sparse wheat residues. Soil samples were taken before and after the experimental period, to perform mineral nitrogen analysis.

Meteorological variables were measured half-hourly: incident and reflected solar radiations (CM7B, Kipp & Zonen, NL), net radiation (NR-Lite, Kipp & Zonen, NL),
20 wind speed (cup anemometer, Cimel, FR) and direction (W200P, Campbell Sci. Inc., USA), air temperature and relative humidity (HMP-45, Vaisala, FI) and precipitations (ARG100, Campbell Sci. Inc., USA). In addition, temperature (copper-constantan thermocouple, OMEGA, UK) and wind-speed (cup anemometer, Cimel, FR) profiles were measured at 0.3, 0.7, 1, 1.4, 2, 2.7, 3.8, 5.3 and 7.5 m above the ground. Soil
25 temperature (copper-constantan thermocouple OMEGA, UK) and soil water content (TDR CS 616, Campbell Sci. Inc., USA) profiles were also measured at 5, 10, 20, 30,

Comparison of methods for the determination of NO-O₃-NO₂ fluxes

P. Stella et al.

Title Page

Abstract

Introduction

Conclusions

References

Tables

Figures

⏪

⏩

◀

▶

Back

Close

Full Screen / Esc

Printer-friendly Version

Interactive Discussion



70 and 90 cm depth and at 5, 10, 20, 30, 50 and 90 cm depth, respectively. TDR probes were calibrated against soil core samples. The photolysis rate for NO_2 (j_{NO_2}) was measured with a filter radiometer (Meteorologie consult GmbH, Germany). In addition, slow response analysers measured O_3 , NO and NO_2 concentrations at 1.6 m (Table 1).

Three methods were used to measure fluxes between the surface and the atmosphere, i.e. aerodynamic gradient (AGM), eddy-covariance (EC) and automatic chambers (CH) methods. The instrument fetches ranged from 100 m to more than 400 m. The footprint analysis reported in Loubet et al. (2011) at 3.17 m height indicated that up to 93 % (average on a 10 days running median) of the field was in the EC mast footprint in spring-summer. Thus, at least 93 % of the field was in the AGM mast footprint since it was lower (see Sect. 2.2) than the EC mast. Each measurement system as well as the flux calculations are explained in the following.

2.2 Aerodynamic gradient measurements

This method was used to determine O_3 -NO- NO_2 fluxes. The O_3 -NO- NO_2 mixing ratio profile measurements consisted of three Teflon PFA (perfluoroalkoxy copolymer) sample lines, each 7 m long with internal diameter of 9.24 mm. The inlets were installed at 0.2, 0.7 and 1.6 m above the ground. The geometric mean measurement height was 0.61 meters. To avoid the condensation of water vapour and avoid photochemical reactions, the sample lines were slightly heated with copper-constantan thermocouples under 12 V tension and protected from radiation, respectively. A flow rate of 40 l min^{-1} in each line was provided by a pump (SV 1010 B, Busch, Switzerland). A subsample line (Teflon PFA, 3.96 mm internal diameter) was connected on each 7 m sample line and connected to a Teflon solenoid valve (NRResearch, USA) allowing to sequentially select a sample line. The switch between each line was performed every 30 s. A purge time of 10 s was used to purge the subsample line and the analysers. The flux inside the sample lines was 7 l min^{-1} . The total lag time of the system was estimated to 1.6 s.

Concentrations were measured with fast chemiluminescent gas analysers for O_3 , NO and NO_2 (Table 1). These instruments were placed in a thermostated box

Comparison of methods for the determination of $\text{NO-O}_3\text{-NO}_2$ fluxes

P. Stella et al.

Title Page

Abstract

Introduction

Conclusions

References

Tables

Figures

⏪

⏩

◀

▶

Back

Close

Full Screen / Esc

Printer-friendly Version

Interactive Discussion



($34.0 \pm 0.5^\circ\text{C}$) (Fig. 1). For NO_2 , an ozone scrubber (Drummond Technology, Canada) was used to suppress the interference of O_3 . The NO and NO_2 fast sensors were calibrated every 6 h with a TPG titration unit (146C, Thermo-Environment, USA). For O_3 , the fast ozone sensor was calibrated every 6 h by regression between measurements of slow and fast ozone sensor at 1.6 m. The flux calculation was performed for time intervals of 30 min. The flux (F_C) of the gas (c) was calculated with the gradient approach (see e.g. Sutton et al., 1993) from friction velocity (u_*) and the concentration scaling parameter (C_*) as:

$$F_C = -u_* C_* \quad (1)$$

where u_* was measured by eddy-covariance (see Sect. 2.3) and C_* is defined from the stability corrected gradient of scalar concentration (C) with height (z) as:

$$C_* = k \frac{\partial C}{\partial (\ln(z-d) - \Psi_H)} \quad (2)$$

where k is the von Karman's constant (0.41), d the displacement height (m) assumed equal to zero for a bare soil and Ψ_H the integrated stability correction function for scalars (Dyer and Hicks, 1970):

$$\Psi_H = -5.2 \frac{z-d}{L_{MO}} \quad \text{in stable conditions } (L_{MO} > 0) \quad (3a)$$

$$\Psi_H = 2 \ln \left(\frac{1 + \left(\left(1 - 16 \frac{z-d}{L_{MO}} \right)^{0.25} \right)^2}{2} \right) \quad \text{in unstable conditions } (L_{MO} < 0) \quad (3b)$$

where L_{MO} (in m) is the Monin-Obukhov length deduced from eddy-covariance measurements (see Sect. 2.3).

The scaling parameter was determined based on the slope between C and $\ln(z-d) - \Psi_H$ using linear regression.

Comparison of methods for the determination of $\text{NO-O}_3\text{-NO}_2$ fluxes

P. Stella et al.

Title Page

Abstract

Introduction

Conclusions

References

Tables

Figures

⏪

⏩

◀

▶

Back

Close

Full Screen / Esc

Printer-friendly Version

Interactive Discussion



Discussion Paper | Discussion Paper | Discussion Paper | Discussion Paper | Discussion Paper

2.3 Eddy-covariance fluxes

Eddy-covariance is a “direct measuring” flux method without application of any empirical constant (Foken, 2008). It has been extensively used to estimate turbulent fluxes of momentum, heat and trace gases (Aubinet et al., 2000; Running et al., 1999; Baldocchi et al., 2001; Dolman et al., 2006; Skiba et al., 2009), and is thus not detailed here. Briefly, the EC mast included a 3-D sonic anemometer (R3, Gill Inc., UK) and an open-path infrared absorption spectrometer for water vapour and CO₂ (IRGA 7500, LiCor, USA) located at 3.17 m height. Data were sampled and recorded at 50 Hz and the flux calculation was performed for 30 min intervals. Flux calculation was assessed following the CarboEurope methodology (Aubinet et al., 2000), which included a WPL (Webb-Pearman-Leuning) correction for LE flux. From these measurements, the friction velocity (u_* in m s^{-1}) and the Monin Obukhov length (L_{MO} in m) were estimated as:

$$u_* = \left(-\overline{u'w'} \right)^{0.5} \quad (4)$$

$$L_{\text{MO}} = \frac{\rho u_*^3}{\text{kg} \left(\left(\frac{-H}{(\overline{T}_a + 273) c_p} \right) + 0.61 E \right)} \quad (5)$$

where w and u are the vertical and the longitudinal components of the wind velocity, respectively, g is the acceleration due to gravity (m s^{-2}), ρ is the air density (kg m^{-3}), c_p is the air specific heat ($\text{J kg}^{-1} \text{K}^{-1}$), T_a is the air temperature ($^{\circ}\text{C}$), H is the sensible heat flux (W m^{-2}) and E is the water vapour flux ($\text{kg m}^{-2} \text{s}^{-1}$). The overbars and the primes denote the time average and the fluctuation term, respectively. The O₃ flux was measured by EC using the Ratio Method described in Muller et al. (2010) by operating fast and slow response sensors at 3.17 m height simultaneously (Table 1):

Comparison of methods for the determination of NO-O₃-NO₂ fluxes

P. Stella et al.

Title Page

Abstract

Introduction

Conclusions

References

Tables

Figures

◀

▶

◀

▶

Back

Close

Full Screen / Esc

Printer-friendly Version

Interactive Discussion



$$F_{O_3} = \frac{\overline{w'X'_{O_3}}}{\overline{X_{O_3}}} \cdot [\overline{O_3}] \quad (6)$$

where X_{O_3} is the O_3 fast sensor signal and $[\overline{O_3}]$ is the mean absolute O_3 concentration averaged over 30 min from the slow response sensor.

2.4 Flux uncertainty analysis and detection limits

- 5 One indicator of the AGM flux quality is the gradient signal to noise ratio ($\Delta C/\sigma_C$) which was estimated as the average of the concentration difference between two successive levels, divided by the averaged concentration standard deviation. This parameter evaluates the ability to resolve the vertical mixing ratio gradient based on real data, which integrates the analyser precision and the gradient representativeness over the background concentration fluctuation.

10 The relative uncertainty of the AGM flux was expressed as:

$$\frac{\sigma_{Fc}}{F_c} = \sqrt{\left(\frac{\sigma_{u_*}}{u_*}\right)^2 + \left(\frac{\sigma_{C_*}}{C_*}\right)^2} \quad (7)$$

- 15 where σ represents standard deviations. The standard deviation of u_* was estimated based on the approach of Richardson et al. (2006) derived from the basics equations of turbulence:

$$\frac{\sigma_{u_*}}{u_*} = \left[\left(\frac{2 \cdot \tau_t}{t}\right)^{0.5} \cdot \left(\frac{1 + \left(\overline{w'u'}/\sigma_w \sigma_u\right)^2}{\left(\overline{w'u'}/\sigma_w \sigma_u\right)^2}\right)^{0.5} \right]^{0.5} \quad (8)$$

where τ_t is the integral timescale (i.e. the integral of the auto-correlation function) of the vertical wind velocity, t is the averaging time (1800 s) and σ_w and σ_u are the standard deviations w and u .

Comparison of methods for the determination of NO-O₃-NO₂ fluxes

P. Stella et al.

Title Page

Abstract

Introduction

Conclusions

References

Tables

Figures

⏪

⏩

◀

▶

Back

Close

Full Screen / Esc

Printer-friendly Version

Interactive Discussion



Comparison of methods for the determination of NO-O₃-NO₂ fluxes

P. Stella et al.

Title Page

Abstract

Introduction

Conclusions

References

Tables

Figures

◀

▶

◀

▶

Back

Close

Full Screen / Esc

Printer-friendly Version

Interactive Discussion



The standard deviation of C_* (σ_{C_*}) was determined as the standard deviation of the slope between C and $(\ln(z-d) - \Psi_H)$ by linear regression. However, in order to include the uncertainty in both C and Ψ_H , the linear regression was performed every 30 min on a randomly chosen dataset $[N(C, \sigma_C), \Psi_H(N(u_*, \sigma_{u_*}))]$ with a number of data chosen to represent the number of independent data acquired with the fast sensors (at a frequency smaller than the inverse of the integral time scale τ_1 (Lenschow et al., 1994). Here the integral time scale τ_1 was calculated using Edire software.

The flux detection limit was determined empirically as the sum of the intercept of the linear regression between σ_F and F and the standard deviation of the intercept.

2.5 Flux divergence due to chemical reactions

NO, NO₂ and O₃ are subject to (photo-) chemical reactions, thus leading to chemical sources and sinks of these gases within the layer represented by the measurements. These chemical sources and sinks lead in turn to a vertical flux divergence between the surface and the measurement height, which should be taken into account if one is looking for the ecosystem flux. This is true, for instance, when studying O₃ impacts on plants, since the real O₃ flux experienced by the plant may not be that measured at a certain height above the surface. This is also valid for NO when comparing NO fluxes measured with chambers and those measured with EC or the AGM. According to Remde et al. (1993) and Warneck (2000), the main gas phase reactions for the NO-O₃-NO₂ triad are:



where k_r ($= 44.4 \exp(-1370/(T_a + 273))$) in $\text{ppm}^{-1} \text{s}^{-1}$, e.g. Walton et al., 1997) and j_{NO_2} are the rate coefficient and the photolysis frequency for Reactions (R1) and (R2), respectively.

Comparison of methods for the determination of NO-O₃-NO₂ fluxes

P. Stella et al.

Title Page

Abstract

Introduction

Conclusions

References

Tables

Figures

⏪

⏩

◀

▶

Back

Close

Full Screen / Esc

Printer-friendly Version

Interactive Discussion



A simple method based on mass conservation for NO-O₃-NO₂ triad, proposed by Duyzer et al. (1995), was used to calculate the NO, O₃ and NO₂ flux divergences. This method assumes that the corrected flux can be approximated by the uncorrected flux. According to the simple equations for the flux derived by Lenschow and Delany (1987),

Duyzer et al. (1995) demonstrated that, for heights lower than 4 meters, the general form of the flux divergence is:

$$\left(\frac{\partial F}{\partial z}\right)_z = a \ln(z) + b \quad (9)$$

The factors a for NO₂, NO and O₃ are calculated as:

$$a_{\text{NO}_2} = -a_{\text{NO}} = -a_{\text{O}_3} = -\frac{\phi_H}{k u_*} \left[k_r \left([\overline{\text{NO}}] \cdot F_{\text{O}_3} + [\overline{\text{O}_3}] \cdot F_{\text{NO}} \right) - j_{\text{NO}_2} \cdot F_{\text{NO}_2} \right] \quad (10)$$

where $[\overline{\text{NO}}]$ and $[\overline{\text{O}_3}]$ are concentrations at the geometric mean height of the profile measurements and ϕ_H is the stability correction function for heat. Following Dyer and Hicks (1970) and Webb (1970):

$$\phi_H = \left(1 - 16(z - d)/L_{\text{MO}}\right)^{-1/2} \quad -2 \leq (z - d)/L_{\text{MO}} \leq 0 \quad (11a)$$

$$\phi_H = \left(1 + 5(z - d)/L_{\text{MO}}\right) \quad 0 \leq (z - d)/(z - d) L_{\text{MO}} \leq 1. \quad (11b)$$

As shown by Lenschow and Delany (1987), the flux divergence at higher levels approaches zero. The factor b was calculated for NO₂, NO and O₃ as $b = -a \ln(z_2)$, where $z_2 = 1.6$ m, hence assuming that at $z = 1.6$ m the flux divergence was zero. This assumption was made since measurements at higher heights were not available. The corrected surface fluxes (F_0) are then approximated as:

$$F_0 = F_{z_1} + \int_{z_1}^{z_0} \left(\frac{\partial F}{\partial z}\right)_z dz = F + a z_1 \left(1 + \ln(z_2/z_1)\right). \quad (12)$$

2.6 Turbulent transport and chemical reaction times

The comparison between the turbulent and the chemical time scales indicates if chemical reactions may occur within the transport of chemical species, and, therefore whether these can be treated as passive scalar or not. The turbulent transport time (τ_{trans} in s) between the measurement height (z_m) and the ground surface was simply expressed as the transfer resistance through each layer multiplied by the layer height (Garland, 1977):

$$\tau_{\text{trans}} = R_a(z) \times (z_m - z_0) + R_b \times (z_0 - z_{0'}) \approx R_a(z) \times (z_m - z_0) \quad (13)$$

where $R_a(z)$ (s m^{-1}) is the aerodynamic resistance, calculated following Garland (1977) and z_0 and $z_{0'}$ represent the roughness height for momentum and scalars (m), respectively. The contribution of the quasi-laminar boundary layer ($R_b \times (z_0 - z_{0'})$) was evaluated as being negligible ($1.3\% \pm 0.7\%$), and was therefore neglected. The chemical reaction time for NO-O₃-NO₂ triad (τ_{chem} in s) was evaluated at the measurement height following the approach of Lenschow (1982) as:

$$\tau_{\text{chem}} = 1 / \left[j_{\text{NO}_2}^2 + k_r^2 \left([\overline{\text{O}_3}] - [\overline{\text{NO}}] \right)^2 + 2 j_{\text{NO}_2} k_r \left([\overline{\text{O}_3}] + [\overline{\text{NO}}] + 2 [\overline{\text{NO}_2}] \right) \right]^{0.5} \quad (14)$$

Based on this expression, the chemical depletion times for NO, O₃ and NO₂ were estimated as the asymptotic limits of Eq. (14) when either NO, O₃ or NO₂ concentration was becoming the dominant specie (see also De Arellano and Duynderke, 1992):

$$\tau_{\text{deplNO}} = \frac{1}{k_r \cdot [\overline{\text{O}_3}]} \quad (15a)$$

$$\tau_{\text{deplO}_3} = \frac{1}{k_r \cdot [\overline{\text{NO}}]} \quad (15b)$$

$$\tau_{\text{deplNO}_2} = \frac{1}{j_{\text{NO}_2}} \quad (15c)$$

Comparison of methods for the determination of NO-O₃-NO₂ fluxes

P. Stella et al.

Title Page

Abstract

Introduction

Conclusions

References

Tables

Figures

◀

▶

◀

▶

Back

Close

Full Screen / Esc

Printer-friendly Version

Interactive Discussion



Given τ_{trans} and τ_{chem} , the Damköhler number (DA) is defined as:

$$DA = \frac{\tau_{\text{trans}}}{\tau_{\text{chem}}}. \quad (16)$$

2.7 Automatic chamber flux measurements

The automatic chamber method was used to determine NO emissions from soil. Details can be found in Laville et al. (2011). Briefly, 6 automatic chambers in stainless steel (0.7 m × 0.7 m in area and 0.2 m height) measured continuously NO fluxes. The chambers were closed in sequence for 15 min each. The complete duration of one measurement cycle was therefore 01:30 h. The NO and O₃ concentrations inside the chambers were measured using slow sensors (Table 1). The fluxes of NO without corrections for chemical reactions were calculated as:

$$F_{\text{NO}} = \frac{V}{A} \frac{\partial[\text{NO}]}{\partial t} \quad (17)$$

where F_{NO} is the NO flux, V the chamber headspace volume, A the ground area covered by the chamber and $\partial[\text{NO}]/\partial t$ the time derivative of the NO concentration. The NO flux was determined during the first 3 min after chamber closure. Because of the long residence time of the air in the head space of the chamber, the NO fluxes need to be corrected for reactions with O₃ and NO₂. This was done following Laville et al. (2011), based on measurements of NO, NO₂ and O₃. As the chambers were opaque to solar radiation, only the reaction between NO and O₃ was considered and the photolysis of NO₂ was ignored. The corrected NO flux from chamber method is given as:

$$F_{\text{NO}_{\text{corr}}} = \frac{V}{A} \left(\frac{\partial[\text{NO}]}{\partial t} + k_r \cdot [\text{NO}] \cdot [\text{O}_3] \right). \quad (18)$$

Comparison of methods for the determination of NO-O₃-NO₂ fluxes

P. Stella et al.

Title Page

Abstract

Introduction

Conclusions

References

Tables

Figures

⏪

⏩

◀

▶

Back

Close

Full Screen / Esc

Printer-friendly Version

Interactive Discussion



2.8 Modelled ozone flux over bare soil

In order to compare the measured ozone fluxes with existing literature, the ozone flux was modelled following the resistance analogy (Wesely and Hicks, 2000). The ozone deposition velocity ($V_{d_{O_3}}(z)$) was expressed as:

$$V_{d_{O_3}}(z) = \frac{1}{R_a(z) + R_{b_{O_3}} + R_{soil}} \quad (19)$$

where $R_{b_{O_3}}$ ($s\ m^{-1}$) is the soil quasi-laminar boundary layer resistance for ozone calculated following Garland (1977) and R_{soil} ($s\ m^{-1}$) is the soil resistance for ozone. R_{soil} was calculated using the parameterisation proposed by Stella et al. (2011) as:

$$R_{soil} = R_{soil_{min}} \times e^{(k \times RH_{surf})} \quad (20)$$

$$RH_{surf} = \frac{P_{vap_{surf}}}{P_{sat}(T_{surf})} \times 100 \quad (21)$$

where RH_{surf} is the surface relative humidity at z_0 (the roughness height for scalars), $P_{vap_{surf}}$ the water vapour pressure at z_0 (Pa) and $P_{sat}(T_{surf})$ the saturation vapour pressure at z_0 (Pa). $R_{soil_{min}}$ (set at $21\ s\ m^{-1}$) is the dry soil resistance (i.e. at $RH_{surf} = 0\ %$) and k (set at 0.024) is an empirical coefficient of the exponential function, both calibrated against a range of conditions in Grignon (Stella et al., 2011). The modelled ozone flux to the soil ($F_{soil_{O_3}}$) was obtained as:

$$F_{soil_{O_3}} = -V_{d_{O_3}}(z) \cdot [O_3]_{(z)} \quad (22)$$

Comparison of methods for the determination of NO-O₃-NO₂ fluxes

P. Stella et al.

Title Page

Abstract

Introduction

Conclusions

References

Tables

Figures

◀

▶

◀

▶

Back

Close

Full Screen / Esc

Printer-friendly Version

Interactive Discussion

3 Results

3.1 Overview on meteorological conditions, concentrations and AGM fluxes of O₃, NO and NO₂

The experimental period was quite sunny with global radiation reaching 800 W m⁻² at noon, apart from 24 and 27 August, during which global radiation only reached 400 W m⁻². It rained on 24 August with a cumulated precipitation of 2 mm (Fig. 2a). The period was dry and warm. The relative humidity was around 80 % during night-time and decreased to about 30 % during daytime (Fig. 2b). Air temperature varied between 15 °C during night-time and 25 °C during daytime (Fig. 2c). During the measurement period, the wind blew from Paris from 22 to 24 August and during the night of 25 to 26 August (Fig. 2d). The WFPS (water-filled pore space) in the 0–10 top soil layer was around 29 % during the whole period.

During the measurement campaign, the friction velocity ranged from around 0.03 m s⁻¹ during night-time to around 0.45 m s⁻¹. The friction velocity had a marked daily dynamics. It was at a minimum during night-time, increased during the morning to reach its maximum at noon and then decreased to its minimum during the afternoon. Globally, the end of the measurement campaign (from 26 to 30 August 2009) was characterised by stronger friction velocities than during the first part of the campaign, both during night-time and daytime (Fig. 2e).

The mixing ratios of O₃, NO and NO₂ featured a strong daily and day-to-day variation. The ozone concentrations expectedly increased during the early morning to reach a maximum in the early afternoon. Night-time ozone levels were between 0 and 30 ppb, whereas daytime levels were between 40 and 60 ppb. The O₃ mixing ratio variation between daytime and night-time was larger during the beginning, than towards the end of the experiment. The NO and NO₂ mixing ratio variations were markedly different: the minimum occurred during daytime and the maximum occurred during the early morning (between 05:00 and 07:30 UT) and the early evening (between 20:00 and 22:00 UT) during traffic peaks. The highest NO_x mixing ratios were observed during easterly

Comparison of methods for the determination of NO-O₃-NO₂ fluxes

P. Stella et al.

Title Page

Abstract

Introduction

Conclusions

References

Tables

Figures

⏪

⏩

◀

▶

Back

Close

Full Screen / Esc

Printer-friendly Version

Interactive Discussion



winds, i.e. when air masses originated from the city of Paris. These mixing ratio peaks were less marked for NO than for NO₂, with NO₂ mixing ratio always greater than those of NO (Fig. 2f).

The fluxes of O₃, NO and NO₂ estimated using the aerodynamic gradient method are represented in Fig. 2g. These fluxes were uncorrected for chemical reactions; i.e. directly obtained using Eq. (1). For ozone and NO₂, deposition was observed, whereas NO was emitted from the ground. The ozone flux showed a marked day cycle. It increased during the early morning to reach a maximum at noon and then decreased to nearly zero during night. The NO flux was small during most of the measurement campaign, and peaked on 24 August and 25 August following the rain event. The NO₂ flux had a less clear dynamics with alternating increases and decreases in the flux (Fig. 2g).

3.2 Concentration gradients and AGM flux uncertainties

Nitric oxide (NO) concentrations measured with slow and fast sensors agreed very well with a very weak difference of less than 1 % over the whole period (Fig. 3). On the contrary, NO₂ concentrations measured with the slow sensor were systematically higher, up to 25 % in mean over the whole period, than those measured with the fast sensor (Fig. 3).

Ozone mixing ratio gradients were quite large with a mixing ratio difference between the two highest levels ranging generally from 0.35 ppb to 1.65 ppb and between the two lowest levels ranging from 0.7 ppb to 2.4 ppb. The mixing ratio differences were smaller for NO and NO₂ with only around 0.15 ppb, although they could reach 0.35 ppb and 0.8 ppb for NO and NO₂, respectively. However, O₃ and NO₂ concentrations increased with height indicating deposition fluxes on average, whereas NO mixing ratio decreased with height indicating an emission flux on average (Table 2).

The “gradient signal to noise ratio” $\Delta C/\sigma_C$ showed a diurnal dynamics for the three gases: this ratio was higher during night-time and decreased during daytime, following the change in turbulent mixing. However, for ozone, this ratio was systematically

Comparison of methods for the determination of NO-O₃-NO₂ fluxes

P. Stella et al.

Title Page

Abstract

Introduction

Conclusions

References

Tables

Figures

⏪

⏩

◀

▶

Back

Close

Full Screen / Esc

Printer-friendly Version

Interactive Discussion



greater than 1, whereas for NO and NO₂ it was generally below 1 during daytime (except from 24 to 26 August for NO) and larger than 1 at night (Fig. 4).

The relative uncertainty of the AGM fluxes decreased exponentially with increasing friction velocity (Fig. 5). The relative flux uncertainties ranged from 150–200 % for the lowest u_* to around 20 %, 30 % and 40 % for O₃, NO₂ and NO, respectively, for the highest u_* . The relative u_* uncertainty ranged from 90 % to 15 % whereas C_* relative uncertainty varied from 110 % to 5 %, 25 % and 35 % for O₃, NO₂ and NO, respectively.

Based on the standard deviation of the flux, the flux detection limit was estimated as 0.08 nmol m⁻² s⁻¹ for O₃, 0.33 nmol m⁻² s⁻¹ for NO₂ and 0.22 nmol m⁻² s⁻¹ for NO.

3.3 Flux divergences due to chemical reactions

The surface fluxes calculated using Eq. (12) were higher than those at the measurement height for NO and NO₂, whereas they were lower for O₃. Although the magnitude of flux difference was the same for the three trace gases, the NO, NO₂ and O₃ fluxes were not affected in the same extent in terms of percentages. The mean flux correction over the whole campaign was estimated to be less than 1 %, 8 % and 10 % for O₃, NO₂ and NO, respectively. For the latter two trace gases the flux difference increased markedly and could reach up to 80 % when the Damköhler number became greater than unity (see Fig. 6). Such conditions typically occurred between 19:00 and 04:30 UT.

The comparison between the chemical reaction time of the NO-O₃-NO₂ triad and the chemical depletion times for NO, O₃ and NO₂ showed that τ_{chem} was particularly close to τ_{deplNO} whereas τ_{deplO_3} and τ_{deplNO_2} were systematically greater than τ_{chem} (Fig. 7).

Comparison of methods for the determination of NO-O₃-NO₂ fluxes

P. Stella et al.

Title Page

Abstract

Introduction

Conclusions

References

Tables

Figures

⏪

⏩

◀

▶

Back

Close

Full Screen / Esc

Printer-friendly Version

Interactive Discussion

4 Discussion

4.1 Quality of NO-O₃-NO₂ AGM fluxes

One critical point when using the aerodynamic gradient method is to measure the concentrations of gases at different height with sufficient accuracy and precision. Nitric oxide mixing ratios measured with the fast response analyzer agreed very well with the slow response analyzer, whereas NO₂ mixing ratios from the slow response sensor were larger than with the fast response sensor (Fig. 3). The slow sensor uses a molybdenum converter heated at 325 °C to convert NO₂ to NO and evaluates NO₂ mixing ratio by the difference between NO_x and NO mixing ratios. This catalytic conversion is unfortunately not specific to NO₂. Several compounds as peroxyacetyl nitrate (PAN), nitrous acid (HONO), HNO₃ and organic nitrates are also converted to NO and therefore induce an overestimation of the NO₂ mixing ratio (Parrish and Fehsenfeld, 2000; Dari-Salisburgo et al., 2009). The interference using a molybdenum converter could be as large as 50 % of the apparently measured NO₂ concentration in some reported studies (Dunlea et al., 2007). The fast NO₂ sensor measures the chemiluminescence produced by the reaction between NO₂ and an alkaline luminal solution. The only interference reported is with O₃, quoted as less than 1 %, and PAN, quoted at 25 % of the equivalent concentration of NO₂ (Nikitas et al., 1997). However, the fast NO₂ analyser was used with an O₃ scrubber, and the fact that the analyser with the molybdenum sensor gave larger concentrations rather suggests that the slow sensor was subject to positive interferences, probably due to the presence of other reactive nitrogen species (NO_y).

The gradient system was able to measure with a sufficient accuracy the O₃ mixing ratio gradient, as shown by the gradient signal to noise ratio ($\Delta C/\sigma_C$), which was always higher than unity. On the contrary, the NO and NO₂ mixing ratio gradient measurements were generally very close to or below the detection limit, except during night-time and during the NO flux peak (Fig. 4). This larger noise in the NO and NO₂ gradients was both due to a combination of small fluxes (Fig. 2) and large local advection of NO

Comparison of methods for the determination of NO-O₃-NO₂ fluxes

P. Stella et al.

Title Page

Abstract

Introduction

Conclusions

References

Tables

Figures

◀

▶

◀

▶

Back

Close

Full Screen / Esc

Printer-friendly Version

Interactive Discussion



and NO_2 from the nearby traffic lines. Indeed, since the lifetime of ozone is greater than these of NO_x (Logan, 1983), the ozone concentration as a secondary pollutant is expected to show smaller fluctuations than NO and NO_2 .

The relative uncertainty of O_3 , NO and NO_2 fluxes was dependent on the friction velocity and ranged from 150–200 % to 20 %, 40 % and 30 % respectively (Fig. 5). Flux relative uncertainties were mainly due to u_* uncertainty, on the one hand through its contribution to σ_{u_*}/u_* and on the other hand through its contribution to the scaling parameter error (i.e. in the Ψ_H function through Monin-Obukhov length estimation). It is noticeable that the O_3 flux uncertainty was near two times lower than the NO and NO_2 flux uncertainties when u_* was large (typically daytime conditions). This can be explained by the precision of the O_3 mixing ratio gradient compared to NO and NO_2 gradients. During daytime, the O_3 flux was large, which led to a large mixing ratio gradients ($\Delta C/\sigma_C > 1$), as opposed to the NO and NO_2 mixing ratio gradients which were much smaller. On the opposite, during night-time, the uncertainties of the gradient are small and of similar magnitude for the three gases (Fig. 4), but in this case, the flux uncertainty is dominated by the uncertainty on u_* which affects both terms σ_{u_*}/u_* and σ_C/C_* of Eq. (7).

The large number of concentration points available to evaluate the concentration at each level using fast sensors is beneficial in diminishing the flux uncertainty. Figure 8a shows indeed that the relative flux uncertainty diminishes with the number of measurements points per level over a 30 min period. In the present study, the use of fast response sensor provided approximately 2000 measurements per level per 30 min. However, Fig. 8a is constructed assuming that all points are independent (any cross-correlation between the data is equal to zero). Since by definition, the integral time scale τ_1 is the time over which the turbulent signal is correlated to itself (Lenschow et al., 1994), the number of independent points to be considered are those points sampled at a frequency $f_1 = \tau_1^{-1}$. In the example considered in Fig. 8a, the number of point was evaluated as 327 per level per 30 min. The resulting relative flux uncertainty is quite close to the minimal one, i.e. around 30 % for the example considered. Under the

Comparison of methods for the determination of $\text{NO-O}_3\text{-NO}_2$ fluxes

P. Stella et al.

Title Page

Abstract

Introduction

Conclusions

References

Tables

Figures

⏪

⏩

◀

▶

Back

Close

Full Screen / Esc

Printer-friendly Version

Interactive Discussion

Comparison of methods for the determination of NO-O₃-NO₂ fluxes

P. Stella et al.

Title Page

Abstract

Introduction

Conclusions

References

Tables

Figures

⏪

⏩

◀

▶

Back

Close

Full Screen / Esc

Printer-friendly Version

Interactive Discussion

hypothesis of the use of slow response sensor, only 40 measurements per level per 30 min would be available, which corresponded to a relative flux uncertainty ranging from 35 % up to 40 %. In addition, the term σ_{u_x}/u_x is constant and was equal to 30 % in the example considered, and the term σ_{C_x}/C_x is equal to 10 % to 20 % for 40 measurements per level per 30 min and equal to 5 % for 327 measurements per level per 30 min. Thus, the use of fast sensor allowed to diminish the relative C_x uncertainty by a factor 2 to 4 for the example considered here. However, over the whole campaign, the use fast response sensor was only beneficial during daytime when friction velocity was high and the integral time scale was small (Fig. 8b). From the overall look at the dataset, we find that an acquisition frequency of around 1.2 Hz would have been optimum in our case (Fig. 8b). This conclusion would change depending on the average u_x at the site studied.

4.2 Influence of chemical reactions

In contrary to inert gases such as CO₂ and H₂O, the fluxes of reactive species in the surface boundary layer may diverge with height. In the case of the NO-O₃-NO₂ triad, this was shown in previous studies (Kramm et al., 1996; Walton et al., 1997). In addition, the specific chemistry between NO_x and O₃ induces a mass conservation leading to height invariant-fluxes for NO_x (NO + NO₂) and O_x (NO₂ + O₃) species (Kramm et al., 1996; Walton et al., 1997). Although the absolute magnitude of the flux divergence was similar for NO, NO₂ and O₃, the relative correction was very different. The correction of ozone flux was typically negligible (around 1 % in mean), whereas for NO and NO₂ it reached 10 % and 8 % in mean, respectively. The same result were reported by Galmarini et al. (1997) during an experimental study, for which there was no substantial difference between O₃ and inert species fluxes, whereas NO and NO₂ flux divergence were strongly affected by chemistry. This is due to the magnitude of each flux. Indeed, the ozone flux (mean: $-4.27 \text{ nmol m}^{-2} \text{ s}^{-1}$) was ten times higher than the NO and NO₂ fluxes (mean: 0.41 and $-0.33 \text{ nmol m}^{-2} \text{ s}^{-1}$, respectively).

Comparison of methods for the determination of NO-O₃-NO₂ fluxes

P. Stella et al.

Title Page

Abstract

Introduction

Conclusions

References

Tables

Figures

⏪

⏩

◀

▶

Back

Close

Full Screen / Esc

Printer-friendly Version

Interactive Discussion



At the half-hourly time scale, the flux divergence was highly variable and could reach 25% for O₃ and up to 80% for NO and NO₂ (Fig. 6a to c). The flux divergence for the three gases was dependent on the Damköhler number. The chemical reaction time was similar to the chemical depletion time for NO, whereas the chemical depletion times for NO₂ and O₃ were systematically higher (Fig. 7). This result demonstrated that the flux divergence was due to the reaction between NO and O₃ and was limited by NO whose mixing ratio was the lowest, and was not caused by NO₂ photolysis. During the campaign, O₃ concentrations ranged between 15 ppb ($\sim 6.2 \times 10^2 \text{ nmol m}^{-3}$) and 60 ppb ($\sim 24.9 \times 10^2 \text{ nmol m}^{-3}$), whereas NO concentrations only ranged between 1 ppb ($\sim 0.4 \times 10^2 \text{ nmol m}^{-3}$) and 10 ppb ($\sim 4.2 \times 10^2 \text{ nmol m}^{-3}$) (Fig. 2f). In addition, the reaction between NO and O₃ is a second order reaction but could be defined as a pseudo-first order reaction when one of the two compounds is available in excess. Since O₃ was in excess compared to NO in this study, the reaction between NO and O₃ could be assumed as a pseudo first order reaction and a new pseudo first order reaction rate constant for this reaction could be defined as $k'_r = k_r \cdot [\overline{\text{O}_3}]$ (in s⁻¹).

The flux divergence sharply increased, especially for NO and NO₂, when the Damköhler number became greater than 1, i.e. when turbulent transport was slower than chemical reactions (Fig. 5a to c). This typically occurred during night-time, when the friction velocity was very low. Chemistry between NO and O₃ could occur and thus induce a flux divergence due to chemical reactions. For $DA \ll 1$ (i.e. when turbulent transport is much faster than the chemical transformation time), chemistry did not influence the flux. We have considered the concentrations at the mean geometrical height to calculate τ_{chem} , which was not representative of surface conditions. This fact could explain the remaining divergence when $DA \ll 1$, in particular for NO₂ fluxes. Indeed, although the Damköhler number was lower than 1, the surface flux was still different than the flux measured by AGM. In the case of NO₂, the flux correction ranged between 0% and 25% (Fig. 6c). Near the ground, O₃ concentrations were lower and NO concentrations higher than those at the mean geometrical height. Thus, NO emitted from soil could rapidly react with O₃ to form NO₂, which induced a divergence in O₃,

NO and NO₂ fluxes near the ground.

4.3 Comparison of AGM fluxes with EC O₃ and automatic chambers NO fluxes

There are only few studies reporting comparisons of measurement methods, especially for O₃ and NO_x, and most of them do not account for the chemical flux divergence.

Ozone fluxes measured using aerodynamic gradient method showed a reasonable agreement with ozone fluxes measured by eddy-covariance (Fig. 9a). Over the whole period, the difference between EC and AGM ozone fluxes was only about 4 %, which is in the range of the O₃ flux uncertainty. However for the lowest fluxes, i.e. smaller than $-2 \text{ nmol m}^{-2} \text{ s}^{-1}$, ozone fluxes from eddy-covariance measurements were smaller compared to AGM fluxes. These conditions typically corresponded to night-time when small u_* occurred. It is well recognized that eddy-covariance method underestimates fluxes during nocturnal conditions with low u_* (Goulden et al., 1996; Gu et al., 2005; Moureaux et al., 2006). Many reasons, such as drainage and intermittent turbulent transfer in time and space (Massman and Lee, 2002), could explain the underestimation of ozone fluxes using the EC method, leading to the discrepancy with the AGM flux measurements. It is also very well known that AGM fluxes are subject to large uncertainties under stable conditions (Foken, 2008).

The comparison between NO fluxes measured using automatic chambers and AGM method showed a good correlation. However, NO fluxes measured by chambers were nearly five times smaller than those measured by AGM during the large NO emission peak between 24 and 26 August 2009 without corrections for chemical reactions (Fig. 10). Chemical reactions explained only a part of this discrepancy. Indeed, although chemical corrections were included in the flux calculation, the fluxes estimated from chambers were three times lower than those measured by AGM during the large NO emission between 24 and 26 August 2009 (Fig. 10). In addition to chemical reactions in the chamber, other reasons could explain the difference between NO fluxes measured by chambers and AGM methods. On the one hand, it is well known that NO emissions are quite heterogeneous as shown by the large difference between maximal

Comparison of methods for the determination of NO-O₃-NO₂ fluxes

P. Stella et al.

Title Page

Abstract

Introduction

Conclusions

References

Tables

Figures

⏪

⏩

◀

▶

Back

Close

Full Screen / Esc

Printer-friendly Version

Interactive Discussion



canopies such forest (Zhang et al., 2002, 2006) but similar to $V_{d_{O_3}}$ over bare soil (Stella et al., 2011).

The NO_2 deposition was ten times lower than ozone fluxes, with average flux of $-0.33 \text{ nmol m}^{-2} \text{ s}^{-1}$. As for ozone fluxes, NO_2 fluxes are highly dependent on atmospheric NO_2 mixing ratio which lead to highly variables fluxes according to season and regions. Previous studies reported variables NO_2 deposition fluxes: Fang and Mu (2007) found NO_2 fluxes of -0.08 and $-0.05 \text{ nmol m}^{-2} \text{ s}^{-1}$ for cabbage and soybean fields, respectively, for air NO_2 concentrations around 2 ppb while Pilegaard et al. (1998) reported fluxes reaching $-4.3 \text{ nmol m}^{-2} \text{ s}^{-1}$ over an harvested wheat field under air concentrations reaching 50 ppb. Similarly to our study, Butterbach-Bahl et al. (2002) reported NO_2 fluxes around $-0.5 \text{ nmol m}^{-2} \text{ s}^{-1}$ in mean and ranging from -0.17 to $-1.23 \text{ nmol m}^{-2} \text{ s}^{-1}$ for NO_2 concentrations around 5 ppb. In terms of deposition velocity, $V_{d_{NO_2}}$ ranged from 0.2 cm s^{-1} during nighttime to 0.55 cm s^{-1} during daytime. Pilegaard et al. (1998) reported maximal daily $V_{d_{NO_2}}$ about 0.35 cm s^{-1} and Zhang et al. (2005) found $V_{d_{NO_2}}$ ranging from 0.1 cm s^{-1} to 0.45 cm s^{-1} according to the season. The surface resistance for NO_2 found during this experiment ranged from 200 to 800 s m^{-1} , but no visible dynamics appeared during the campaign. These values were in agreement with surface resistances reported by Watt et al. (2004) for turfgrass, ranging from 300 to 700 s m^{-1} , but quite low compared to those proposed by Wesely (1989) for terrestrial ecosystems (from 270 to 3800 s m^{-1}).

The soil NO emission was generally close to zero due to the dry soil condition (WFPS around 29%), except following the small rainfall event which increased the soil NO emission up to $5 \text{ nmol m}^{-2} \text{ s}^{-1}$. The NO emissions fluxes during this period were similar to previous studies: Li and Wang (2007) reported NO emission fluxes varying between 2 and $7 \text{ nmol m}^{-2} \text{ s}^{-1}$ for cabbage field, and Laville et al. (2005) reported fluxes of $0.5 \text{ nmol m}^{-2} \text{ s}^{-1}$ in mean and reaching $12.5 \text{ nmol m}^{-2} \text{ s}^{-1}$ after fertilization for the same site.

Comparison of methods for the determination of NO-O₃-NO₂ fluxes

P. Stella et al.

[Title Page](#)[Abstract](#)[Introduction](#)[Conclusions](#)[References](#)[Tables](#)[Figures](#)[⏪](#)[⏩](#)[◀](#)[▶](#)[Back](#)[Close](#)[Full Screen / Esc](#)[Printer-friendly Version](#)[Interactive Discussion](#)

5 Summary and conclusions

The study reports measurements of NO, O₃ and NO₂ fluxes using the aerodynamic gradient method. The mixing ratio profile measurements were done using fast response sensors. The experiment was performed over an agricultural field during a period with bare soil, from 20 to 30 August 2009. The aim of this study was to evaluate flux measurements using the AGM, to understand to which extent NO, O₃ and NO₂ fluxes were affected by chemical reactions and to compare them to results from dynamic chambers and the EC method.

The comparison of concentrations measured with slow and fast response sensors showed a good agreement between the instruments, except for NO₂. The conversion of NO₂ to NO using a molybdenum converter heated at 325 °C is not specific to NO₂ explaining the observed overestimation of the slow sensor.

The AGM flux uncertainties were mainly due to friction velocity. The relative flux uncertainties ranged from 150–200 % for the lowest u_* to around 20 %, 30 % and 40 % for O₃, NO₂ and NO, respectively, for the highest u_* . However, the use of a fast sensor allowed to diminish the uncertainty. Flux detection limits of the AGM of 0.08 nmol m⁻² s⁻¹ for O₃, 0.33 nmol m⁻² s⁻¹ for NO₂ and 0.22 nmol m⁻² s⁻¹ for NO were estimated.

Flux divergences due to chemical reactions were only 1 % for O₃, but around 10 % for NO and NO₂. In addition, the flux divergence of NO and NO₂ increased when the chemical time scale became smaller than the turbulent transport time and could reach 80 %. It was evaluated that the flux divergence was due to the reaction between NO and O₃, where NO was the limiting compound, and was not caused by the NO₂ photolysis. This study showed that above a bare soil, when ozone fluxes are particularly stronger than NO and NO₂ fluxes, the impact of chemistry upon ozone fluxes could be neglected, in contrary to NO and NO₂ fluxes.

The comparison of the measurement methods showed that the aerodynamic gradient and eddy-covariance methods provided similar O₃ fluxes except during nighttime conditions with low friction velocities affecting both EC and AGM fluxes measurements.

Comparison of methods for the determination of NO-O₃-NO₂ fluxes

P. Stella et al.

Title Page

Abstract

Introduction

Conclusions

References

Tables

Figures

⏪

⏩

◀

▶

Back

Close

Full Screen / Esc

Printer-friendly Version

Interactive Discussion



The NO fluxes determined with the dynamic chamber method were lower than those obtained by the AGM, due to heterogeneous soil NO emissions and a probable perturbation of the soil surface by the presence of chambers.

Thus, this study showed that, contrary to the comparison reported by Muller et al. (2010), the ozone fluxes measured by AGM and EC are reliable, supporting the results obtained by Keronen et al. (2003). According to the results obtained, it is recommended to use specific gas analyzers and to use fast response sensors to limit the uncertainty in flux measurements using profile methods.

Acknowledgements. This work was supported by the French-German project PHOTONA (CNRS/INSU/DFG), the French regional funding R2DS (région Ile-de-France), the French national project Vulnoz (ANR, VMC) and the European program NitroEurope-IP. The authors are very grateful for the suggestions of Christof Amman and Jan Duyzer. The authors gratefully acknowledge Olivier Fanucci and Michel Burban for their help in the field and in the workshop, Bernard Defranssu, Dominique Tristan and Jean-Pierre de Saint-Stéban from the experimental farm of Grignon are also greatly acknowledged for leaving the access to their field.

References

- Ainsworth, E. A.: Rice production in a changing climate: a meta-analysis of responses to elevated carbon dioxide and elevated ozone concentration, *Global Change. Biol.*, 14, 1642–1650, 2008.
- Altimir, N., Tuovinen, J. P., Vesala, T., Kulmala, M., and Hari, P.: Measurements of ozone removal by Scots pine shoots: calibration of a stomatal uptake model including the non stomatal component, *Atmos. Environ.*, 38, 2387–2398, 2004.
- Altimir, N., Kolari, P., Tuovinen, J.-P., Vesala, T., Bäck, J., Suni, T., Kulmala, M., and Hari, P.: Foliage surface ozone deposition: a role for surface moisture?, *Biogeosciences*, 3, 209–228, doi:10.5194/bg-3-209-2006, 2006.
- Aneja, V. P. and Robarge, W. P.: Soil-biogenic NO_x, emissions and air quality, in: *Preservation of Our World in the Wake of Change*, vol. VIA, edited by: Steinberger, Y., Israel Society for Ecology, 50–52, 1996.

Comparison of methods for the determination of NO-O₃-NO₂ fluxes

P. Stella et al.

Title Page

Abstract

Introduction

Conclusions

References

Tables

Figures

⏪

⏩

◀

▶

Back

Close

Full Screen / Esc

Printer-friendly Version

Interactive Discussion



Comparison of methods for the determination of NO-O₃-NO₂ fluxes

P. Stella et al.

Title Page

Abstract

Introduction

Conclusions

References

Tables

Figures

◀

▶

◀

▶

Back

Close

Full Screen / Esc

Printer-friendly Version

Interactive Discussion



Aubinet, M., Grelle, A., Ibrom, A., Rannik, U., Moncrieff, J., Foken, T., Kowalski, A. S., Martin, P. H., Berbigier, P., Bernhofer, C., Clement, R., Elbers, J., Granier, A., Grunwald, T., Morgenstern, K., Pilegaard, K., Rebmann, C., Snijders, W., Valentini, R., and Vesala, T.: Estimates of the annual net carbon and water exchange of forests: The EUROFLUX methodology, *Adv. Ecol. Res.*, 30, 113–175, 2000.

Baldocchi, D. D., Falge, E., Gu, L., Olson, R., Hollinger, D., Running, S., Anthoni, P., Bernhofer, C., Davis, K., Evans, R., Fuentes, J., Goldstein, A., Katul, G., Law, B., Lee, X., Malhi, Y., Meyers, T., Munger, W., Oechel, W., Paw U, K. T., Pilegaard, K., Schmid, H. P., Valentini, R., Verma, S., Vesala, T., Wilson, K., and Wofsy, S.: FLUXNET: A New Tool to Study the Temporal and Spatial Variability of Ecosystem-Scale Carbon Dioxide, Water Vapor and Energy Flux Densities, *B. Am. Meteorol. Soc.*, 82, 2415–2434, 2001.

Bassin, S., Calanca, P., Weidinger, T., Gerosa, G., and Fuhrer, J.: Modeling seasonal ozone fluxes to grassland and wheat: model improvement, testing, and application, *Atmos. Environ.*, 38, 2349–2359, 2004.

Butterbach-Bahl, K., Breuer, L., Gasche, R., Willibald, G., and Papen, H.: Exchange of trace gases between soils and the atmosphere in Scots pine forest ecosystems of the northeastern German lowlands, 1. Fluxes of N₂O, NO/NO₂ and CH₄ at forest sites with different N-deposition, *Forest Ecol. Manage.*, 167, 123–134, 2002.

Cieslik, S.: Ozone fluxes over various plant ecosystems in Italy: a review, *Environ. Pollut.*, 157, 1487–1496, 2009.

Coe, H., Gallagher, M. W., Choularton, T. W., and Dore, C.: Canopy scale measurements of stomatal and cuticular O₃ uptake by sitka spruce, *Atmos. Environ.*, 29, 1413–1423, 1995.

Coyle, M., Nemitz, E., Storeton-West, R., Fowler, D., and Cape, J. N.: Measurements of ozone deposition to a potato canopy, *Agr. Forest Meteorol.*, 149, 655–666, 2009.

Dari-Salisburgo, C., Di Carlo, P., Giammaria, F., Kajii, Y., and D'Altorio, A.: Laser induced fluorescence instrument for NO₂ measurements: Observations at a central Italy background site, *Atmos. Environ.*, 43, 970–977, 2009.

De Arellano, J. V. G. and Duykerke, P. G.: Influence of chemistry on the flux-gradient relationships for the NO-O₃-NO₂ system, *Bound.-Lay. Meteorol.*, 61, 375–387, 1992.

De Arellano, J. V. G., Duykerke, P. G., and Builtjes, P. J. H.: The divergence of the turbulent diffusion flux in the surface layer due to chemical reactions: the NO-O₃-NO₂ system, *Tellus B*, 45, 23–33, 1993.

Comparison of methods for the determination of NO-O₃-NO₂ fluxes

P. Stella et al.

Title Page

Abstract

Introduction

Conclusions

References

Tables

Figures

⏪

⏩

◀

▶

Back

Close

Full Screen / Esc

Printer-friendly Version

Interactive Discussion



- Delmas, R., Serça, D., and Jambert, C.: Global inventory of NO_x sources, *Nutr. Cycl. Agroecosys.*, 48, 51–60, 1997.
- Denman, K. L., Brasseur, G., Chidthaisong, A., Ciais, P., Cox, P. M., Dickinson, R. E., Hauglustaine, D., Heinze, C., Holland, E., Jacob, D., Lohmann, U., Ramachandran, S., da Silva Dias, P. S., Wofsy, S. C., and Zhang, X.: Climate Change 2007: The Physical Science Basis, Contribution of Working Group I to the Fourth Assessment Report of the Intergovernmental Panel on Climate Change, Couplings between changes in the climate system and biogeochemistry, edited by: Solomon, S., Qin, D., Manning, M., Chen, Z., Marquis, M., Averyt, K. B., Tignor, M., and Miller, H. L., Cambridge University Press, Cambridge, UK, and New York, NY, USA, 2007.
- Denmead, O. T.: Approaches to measuring fluxes of methane and nitrous oxide between landscape and the atmosphere, *Plant Soil.*, 309, 5–24, 2008.
- Dolman, A. J., Noilhan, J., Durand, P., Sarrat, C., Brut, A., Pignatelli, B., Butet, A., Jarosz, N., Brunet, Y., Loustau, D., Lamaud, E., Tolck, L., Ronda, R., Miglietta, F., Gioli, B., Magliulo, V., Esposito, M., Gerbig, C., Körner, S., Glademard, P., Ramonet, M., Ciais, P., Neininger, B., Hutjes, R. W. A., Elbers, J. A., Macatangay, R., Schrems, O., Pérez-Landa, G., Sanz, M. J., Scholz, Y., Facon, G., Ceschia, E., and Beziat, P.: The CarboEurope regional experiment strategy, *B. Am. Meteorol. Soc.*, 87, 1367–1379, 2006.
- Dunlea, E. J., Herndon, S. C., Nelson, D. D., Volkamer, R. M., San Martini, F., Sheehy, P. M., Zahniser, M. S., Shorter, J. H., Wormhoudt, J. C., Lamb, B. K., Allwine, E. J., Gaffney, J. S., Marley, N. A., Grutter, M., Marquez, C., Blanco, S., Cardenas, B., Retama, A., Ramos Villegas, C. R., Kolb, C. E., Molina, L. T., and Molina, M. J.: Evaluation of nitrogen dioxide chemiluminescence monitors in a polluted urban environment, *Atmos. Chem. Phys.*, 7, 2691–2704, doi:10.5194/acp-7-2691-2007, 2007.
- Duyzer, J. H., Deinum, G., and Baak, J.: The interpretation of measurements of surface exchange of nitrogen oxides: correction for chemical reactions, *Philos. T. Roy. Soc. A*, 351, 231–248, 1995.
- Dyer, A. J. and Hicks, B. B.: Flux-profile relationship in the constant flux layer, *Q. J. Roy. Meteorol. Soc.*, 96, 715–721, 1970.
- Fang, S. and Mu, Y.: NO_x fluxes from the three kinds of agricultural lands in the Yangtze Delta, China, *Atmos. Environ.*, 41, 4766–4772, 2007.

Comparison of methods for the determination of NO-O₃-NO₂ fluxes

P. Stella et al.

Title Page

Abstract

Introduction

Conclusions

References

Tables

Figures

◀

▶

◀

▶

Back

Close

Full Screen / Esc

Printer-friendly Version

Interactive Discussion



Fares, S., McKay, M., Holzinger, R., and Goldstein, A. H.: Ozone fluxes in a *Pinus ponderosa* ecosystem are dominated by non-stomatal processes: Evidence from long-term continuous measurements, *Agr. Forest Meteorol.*, 150, 420–431, 2010.

Felzer, B. S., Cronin, T., Reilly, J. M., Melillo, J. M., and Wang, X.: Impacts of ozone on trees and crops, *C. R. Geosci.*, 339, 784–798, 2007.

Foken, T.: *Micrometeorology*, Springer Verlag, Berlin, Heidelberg, p.308, 2008.

Fowler, D., Flechard, C., Skiba, U., Coyle, M., and Cape, J. N.: The atmospheric budget of oxidized nitrogen and its role in ozone formation and deposition, *New. Phytol.*, 139, 11–23, 1998.

10 Fowler, D., Cape, J. N., Coyle, M., Smith, R. I., Hjellbrekke, A. G., Simpson, D., Derwent, R. G., and Jonhson, C. E.: Modelling photochemical oxidant formation, transport, deposition and exposure of terrestrial ecosystems, *Environ. Pollut.*, 100, 43–55, 1999.

Galmarini, S., De Arellano, J. V. G., and Duyzer, J.: Fluxes of chemically reactive species inferred from mean concentration measurements, *Atmos. Environ.*, 31, 2371–2374, 1997.

15 Garland, J. A.: The dry deposition of sulphur dioxide to land and water surface, *P. Roy. Soc. Lond. A*, 354, 245–268, 1997.

Gerosa, G., Marzuoli, R., Cieslik, S., and Ballarin-Denti, A.: Stomatal ozone fluxes over barley field in Italy, “Effective exposure” as a possible link between exposure- and flux-based approaches, *Atmos. Environ.*, 38, 2421–2432, 2004.

20 Gerosa, G., Vitale, M., Finco, A., Manes, F., Ballarin-Denti, A., and Cieslik, S.: Ozone uptake by an evergreen Mediterranean Forest (*Quercus ilex*) in Italy, Part I: Micrometeorological flux measurements and flux partitioning, *Atmos. Environ.*, 39, 3255–3266, 2005.

Gerosa, G., Dergghi, F., and Cieslik, S.: Comparison of different algorithms for stomatal ozone flux determination from micrometeorological measurements, *Water Air Soil Poll.*, 179, 309–321, 2007.

25 Goulden, M. L., Munger, J. W., Fan, S. M., Daube, B. C., and Wofsy, S. C.: Measurements of carbon sequestration b long-term eddy-covariance: methods and critical evaluation of accuracy, *Global Change. Biol.*, 2, 169–182, 1996.

30 Gu, L., Falge, E. M., Boden, T., Baldocchi, D. D., Black, T. A., Saleska, S. R., Suni, T., Verma, S. B., Vesala, T., Wofsy, S. C., and Xu, L.: Objective threshold determination for nighttime eddy flux filtering, *Agr. Forest Meteorol.*, 128, 179–197, 2005.

Comparison of methods for the determination of NO-O₃-NO₂ fluxes

P. Stella et al.

Title Page

Abstract

Introduction

Conclusions

References

Tables

Figures

⏪

⏩

◀

▶

Back

Close

Full Screen / Esc

Printer-friendly Version

Interactive Discussion



- Lenschow, D. H. and Delany, A. C.: An analytic formulation for NO and NO₂ flux profiles in the atmospheric surface layer, *J. Atmos. Chem.*, 5, 301–309, 1987.
- Lenschow, D. H., Mann, J., and Kristensen, L.: How long is long enough when measuring fluxes and other turbulence statistics, *J. Atmos. Ocean. Tech.*, 11, 661–673, 1994.
- 5 Li, D. and Wang, X.: Nitric oxide emission from a typical vegetable field in the Pearl River Delta, China, *Atmos. Environ.*, 41, 9498–9505, 2007.
- Logan, J. A.: Nitrogen oxides in the troposphere: Global and regional budgets, *J. Geophys. Res.*, 88, 785–807, 1983.
- Loubet, B., Laville, P., Lehuger, S., Larmanou, E., Flechard, C., Mascher, N., Genermont, S.,
 10 Roche, R., Ferrara, R. M., Stella, P., Personne, P., Durant, B., Decuq, C., Flura, D., Masson, S., Fanucci, O., Rampon, J. N., Siemens, J., Kindler, R., Gabrielle, B., and Cellier, P.: Carbon, nitrogen and Greenhouse gases budgets over a four years crop rotation in northern France, *Plant Soil*, 343(1–2), 109–137, 2011.
- Massman, W. J. and Lee, X.: Eddy covariance flux corrections and uncertainties in long-term
 15 studies of carbon and energy exchanges, *Agr. Forest Meteorol.*, 113, 121–144, 2002.
- Meixner, F. X., Fickinger, Th., Marafu, L., Serça, D., Nathaus, F. J., Makina, E., Mukurumbira, L., and Andreae, M. O.: Preliminary results on nitric oxide emission from a southern African savanna ecosystem, *Nutr. Cycl. Agroecosys.*, 48, 123–138, 1997.
- Milford, C., Theobald, M. R., Nemitz, E., Hargreaves, K. J., Horvath, L., Raso, J., Dämmgen, U.,
 20 Neftel, A., Jones, S. K., Hensen, A., Loubet, B., Cellier, P., and Sutton, M. A.: Ammonia fluxes in relation to cutting and fertilization of an intensively managed grassland derived from an inter-comparison of gradient measurements, *Biogeosciences*, 6, 819–834, doi:10.5194/bg-6-819-2009, 2009.
- Moureaux, C., Debacq, A., Bodson, B., Heinesch, B., and Aubinet, M.: Annual net ecosystem
 25 carbon exchange by a sugar beet crop, *Agr. Forest Meteorol.*, 139, 25–39, 2006.
- Muller, J. B. A., Coyle, M., Fowler, D., Gallagher, M. W., Nemitz, E. G., and Percival, C. J.: Comparison of ozone fluxes over grassland by gradient and eddy covariance technique, *Atmos. Sci. Lett.*, 10, 164–169, 2009.
- Muller, J. B. A., Percival, C. J., Gallagher, M. W., Fowler, D., Coyle, M., and Nemitz, E.: Sources
 30 of uncertainty in eddy covariance ozone flux measurements made by dry chemiluminescence fast response analysers, *Atmos. Meas. Tech.*, 3, 163–176, doi:10.5194/amt-3-163-2010, 2010.

Comparison of methods for the determination of NO-O₃-NO₂ fluxes

P. Stella et al.

Title Page

Abstract

Introduction

Conclusions

References

Tables

Figures

◀

▶

◀

▶

Back

Close

Full Screen / Esc

Printer-friendly Version

Interactive Discussion



Sanchez-Martin, L., Vallejo, A., Dick, J., and Skiba, U.: The influence of soluble carbon and fertilizer nitrogen on nitric oxide and nitrous oxide emissions from two contrasting agricultural soils, *Soil Biol. Biochem.*, 40, 142–151, 2008.

Sitch, S., Cox, P. M., Collins, W. J., and Huntingford, C.: Indirect radiative forcing of climate change through ozone effects on the land-carbon sink, *Nature*, 448, 791–795, 2007.

Skiba, U., Drewer, J., Tang, Y. S., van Dijk, N., Helfter, C., Nemitz, E., Famulari, D., Cape, J. N., Jones, S. K., Twigg, M., Pihlatie, M., Vesala, T., Larsen, K. S., Carter, M. S., Ambus, P., Ibrom, A., Beier, C., Hensen, A., Frumau, A., Erisman, J. W., Brüggemann, N., Gasche, R., Butterbach-Bahl, K., Neftel, A., Spirig, C., Horvath, L., Freibauer, A., Cellier, P., Laville, P., Loubet, B., Magliulo, E., Bertolini, T., Seufert, G., Andersson, M., Manca, G., Laurila, T., Aurela, M., Lohila, A., Zechmeister-Boltenstern, S., Kitzler, B., Schauffler, G., Siemens, J., Kindler, R., Flechard, C., and Sutton, M. A.: Biosphere-atmosphere exchange of reactive nitrogen and greenhouse gases at the NitroEurope core flux measurements sites: Measurement strategy and first data sets, *Agr. Ecosyst. Environ.*, 133, 139–149, 2009.

Stella, P., Loubet, B., Lamaud, E., Laville, P., and Cellier, P.: Ozone deposition onto bare soil: a new parameterisation, *Agr. Forest. Meteorol.*, 151, 669–681, 2011.

Sutton, M. A., Fowler, D., and Moncrieff, J. B.: The exchange of atmospheric ammonia with vegetated surfaces, I: Unfertilized vegetation, *Q. J. Roy. Meteorol. Soc.*, 119, 1023–1045, 1993.

Vingarzan, R.: A review of surface ozone background levels and trends, *Atmos. Environ.*, 38, 3431–3442, 2004.

Walton, S., Gallagher, M. W., and Duyzer, J. H.: Use of a detailed model to study the exchange of NO_x and O₃ above and below a deciduous canopy, *Atmos. Environ.*, 31, 2915–2931, 1997.

Warneck, P.: *Chemistry of the Natural Atmosphere*, 2nd Edn., International Geophysics Series, Academic Press Inc., San Diego, USA, 2000.

Watt, S. A., Wagner-Riddle, C., Edwards, G., and Vet, R. J.: Evaluating a flux-gradient approach for flux and deposition of nitrogen dioxide over short-grass surfaces, *Atmos. Environ.*, 38, 2619–2626, 2004.

Webb, E. K.: Profile relationships: the log-linear range, and extension to strong stability, *Q. J. Roy. Meteorol. Soc.*, 106, 85–100, 1970.

Comparison of methods for the determination of NO-O₃-NO₂ fluxes

P. Stella et al.

Title Page

Abstract

Introduction

Conclusions

References

Tables

Figures

⏪

⏩

◀

▶

Back

Close

Full Screen / Esc

Printer-friendly Version

Interactive Discussion



- Wesely, M. L.: Parameterization of surface resistances to gaseous dry deposition in regional-scale numerical models, *Atmos. Environ.*, 23, 1293–1304, 1989.
- Wesely, M. L. and Hicks, B. B.: A review of the current status of knowledge on dry deposition, *Atmos. Environ.*, 34, 2261–2282, 2000.
- 5 Wittig, V. E., Ainsworth, E. A., Naidu, S. L., Karnosky, D. F., and Long, S. P.: Quantifying the impact of current and future tropospheric ozone on tree biomass, growth, physiology and biochemistry: a quantitative meta-analysis, *Global Change. Biol.*, 15, 396–424, 2009.
- Yienger, J. J. and Levy, H.: Empirical model of global soil-biogenic NO_x emissions, *J. Geophys. Res.-Atmos.*, 200, 11447–11464, 1995.
- 10 Zhang, L., Brook, J. R., and Vet, R.: On ozone dry deposition with emphasis on non-stomatal uptake and wet canopies, *Atmos. Environ.*, 36, 4787–4799, 2002.
- Zhang, L., Brook, J. R., Vet, R., Wiebe, A., Mihele, C., Shaw, M., O'Brien, J. M., and Iqbal, S.: Estimation of contributions of NO₂ and PAN to Total atmospheric deposition of oxidized nitrogen across Eastern Canada, *Atmos. Environ.*, 39, 7030–7043, 2005.
- 15 Zhang, L., Vet, R., Brook, J. R., and Legge, A. H.: Factors affecting stomatal uptake of ozone by different canopies and a comparison between dose and exposure, *Sci. Total Environ.*, 370, 117–132, 2006.

Comparison of methods for the determination of NO-O₃-NO₂ fluxes

P. Stella et al.

Title Page

Abstract

Introduction

Conclusions

References

Tables

Figures

⏪

⏩

◀

▶

Back

Close

Full Screen / Esc

Printer-friendly Version

Interactive Discussion



Table 1. Instruments used for O₃-NO-NO₂ measurements. The instrument characteristics are those given by the manufacturers.

Measurement method	Gas measured	Analyser	Instrument characteristics	Measurement height	Measurement principle	Measurement frequency
Aerodynamic Gradient Method	O ₃	FOS, Sextant Technology Ltd, New Zealand	Noise (1σ): NA Detection limit (±2σ): NA	0.2, 0.7 and 1.6 m sequentially	Chemiluminescence	5 Hz (fast sensor)
	NO	CLD780TR, Ecophysics, Switzerland	Noise (1σ): <0.5 % of signal or 0.025 ppb Detection limit (±2σ): <0.02 ppb	0.2, 0.7 and 1.6 m sequentially	Chemiluminescence	5 Hz (fast sensor)
	NO ₂	LMA 3D-NO ₂ , Unisearch Associates Inc., Ontario, Canada	Noise (1σ): 1.5 % of signal Detection limit (±2σ): 0.05 ppb	0.2, 0.7 and 1.6 m sequentially	Chemiluminescence	5 Hz (fast sensor)
Eddy-Covariance Method	O ₃	ATDD, NOAA, USA	Noise (1σ): NA Detection limit (±2σ): NA	3.17 m	Chemiluminescence	20 Hz (fast sensor)
	O ₃	O ₃ 41M, Environnement SA, France	Noise (1σ): 0.5 ppb Detection limit (±2σ): 1 ppb	3.17 m	UV absorption	0.1 Hz (slow sensor)
Automatic Chambers Method	NO	42 CTL, Thermo-Environmental Instruments Inc., USA	Noise (1σ): 0.5 ppb Detection limit (±2σ): 1 ppb	Inside the chambers	Chemiluminescence	0.1 Hz (slow sensor)
	O ₃	O ₃ 41M, Environnement SA, France	Noise (1σ): 0.5 ppb Detection limit (±2σ): 1 ppb	Inside the chambers	UV absorption	0.1 Hz (slow sensor)
Other	NO/NO ₂	42i, Thermo-Environmental Instruments Inc., USA	Noise (1σ): 0.4 ppb Detection limit (±2σ): 0.8 ppb	1.6 m	Chemiluminescence	0.1 Hz (slow sensor)
	O ₃	O ₃ 41M, Environnement SA, France	Noise (1σ): 0.5 ppb Detection limit (±2σ): 1 ppb	1.6 m	UV absorption	0.1 Hz (slow sensor)

Comparison of methods for the determination of NO-O₃-NO₂ fluxes

P. Stella et al.

Title Page

Abstract

Introduction

Conclusions

References

Tables

Figures

⏪

⏩

◀

▶

Back

Close

Full Screen / Esc

Printer-friendly Version

Interactive Discussion



Table 2. First quartile, median and third quartile of half-hourly mixing ratio difference measured between 1.6 m and 0.7 m and between 0.7 m and 0.2 m over the entire measurement period for O₃, NO and NO₂.

	Mixing ratio difference between 1.6 m and 0.7 m (ppb)			Mixing ratio difference between 0.7 m and 0.2 m (ppb)		
	O ₃	NO	NO ₂	O ₃	NO	NO ₂
1st Quartile	0.35	-0.3	0	0.7	-0.35	0
Median	1	-0.15	0.05	1.5	-0.15	0.15
3rd Quartile	1.65	-0.05	0.3	2.4	-0.1	0.8

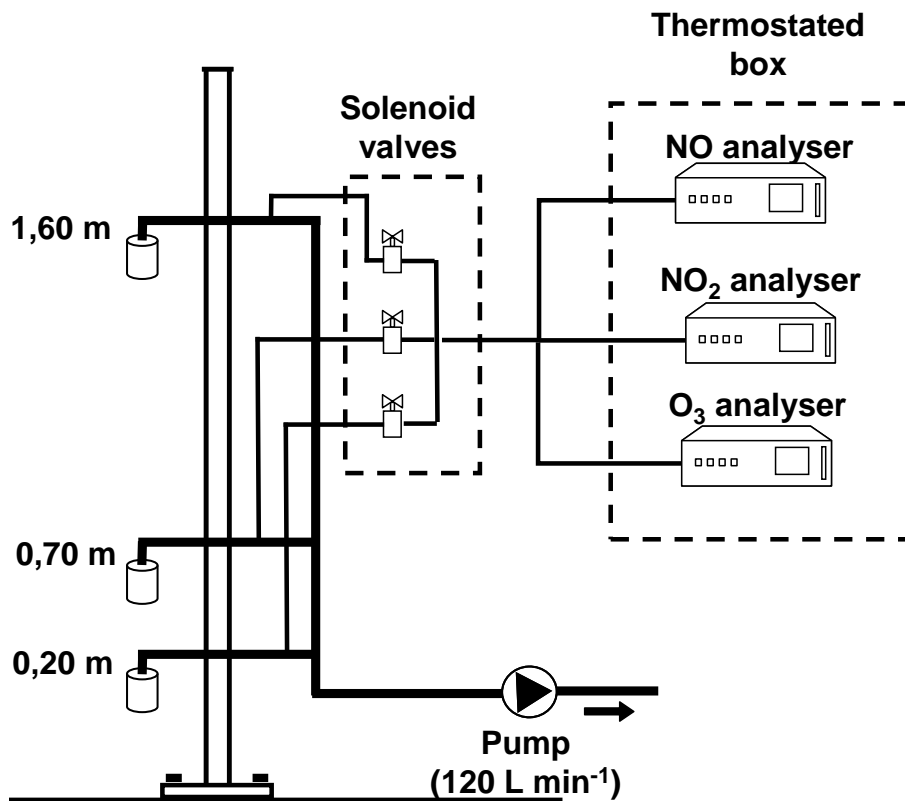


Fig. 1. Measurement set-up for the determination NO-O₃-NO₂ fluxes using aerodynamic gradient method.

Comparison of methods for the determination of NO-O₃-NO₂ fluxes

P. Stella et al.

Title Page	
Abstract	Introduction
Conclusions	References
Tables	Figures
◀	▶
◀	▶
Back	Close
Full Screen / Esc	
Printer-friendly Version	
Interactive Discussion	

Comparison of methods for the determination of NO-O₃-NO₂ fluxes

P. Stella et al.

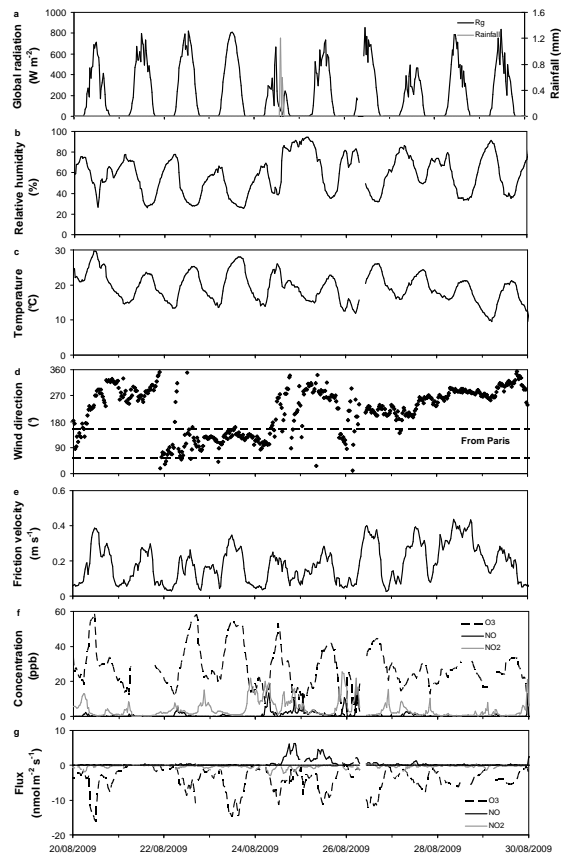


Fig. 2. Time series of **(a)** global radiation (black line) and rainfall (grey line), **(b)** air relative humidity, **(c)** air temperature, **(d)** wind direction, **(e)** friction velocity, **(f)** O₃ (dotted line), NO (black line) and NO₂ (grey line) mixing ratios, and **(g)** O₃ (dotted line), NO (black line) and NO₂ (grey line) fluxes determined by the AGM. The fluxes were calculated without chemical corrections. The dotted lines in panel **(d)** indicate winds coming from Paris.

[Title Page](#)
[Abstract](#)
[Introduction](#)
[Conclusions](#)
[References](#)
[Tables](#)
[Figures](#)
[◀](#)
[▶](#)
[◀](#)
[▶](#)
[Back](#)
[Close](#)
[Full Screen / Esc](#)
[Printer-friendly Version](#)
[Interactive Discussion](#)

Comparison of methods for the determination of NO-O₃-NO₂ fluxes

P. Stella et al.

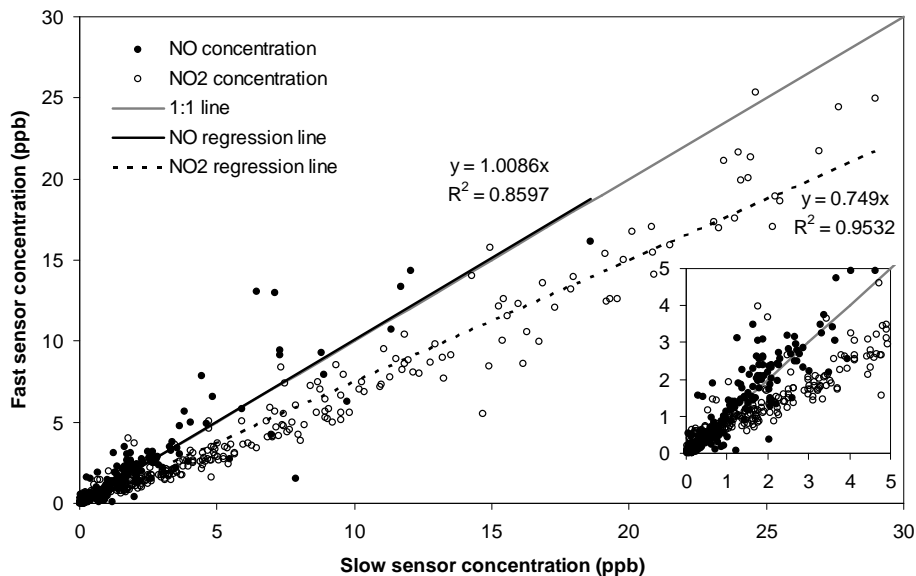


Fig. 3. Comparison of NO (black symbol) and NO₂ (open symbol) mixing ratios measured at 1.6 m height with slow and fast sensors. Grey line is the 1:1 line, black line the regression function for NO and dotted line the regression function for NO₂.

[Title Page](#)[Abstract](#)[Introduction](#)[Conclusions](#)[References](#)[Tables](#)[Figures](#)[◀](#)[▶](#)[◀](#)[▶](#)[Back](#)[Close](#)[Full Screen / Esc](#)[Printer-friendly Version](#)[Interactive Discussion](#)

Comparison of methods for the determination of NO-O₃-NO₂ fluxes

P. Stella et al.

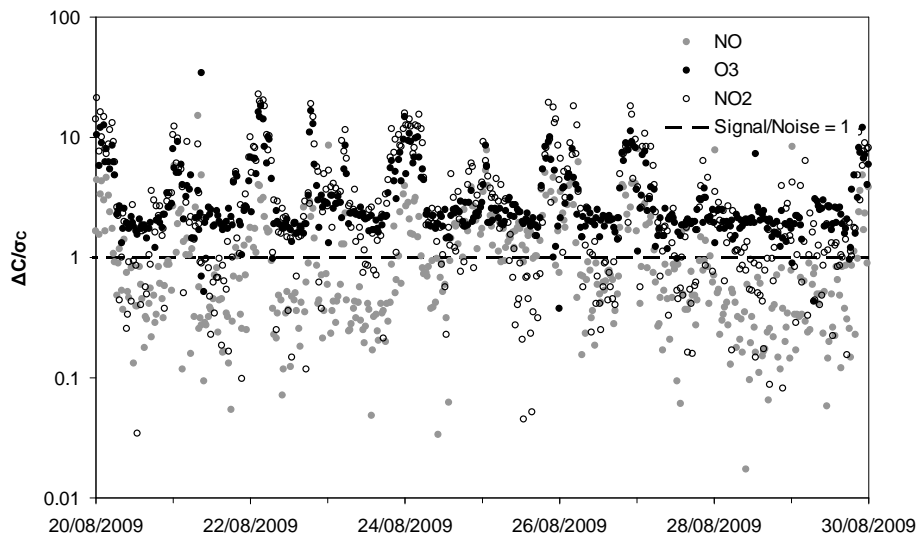


Fig. 4. Time series of the gradient signal to noise ratio ($\Delta C/\sigma_C$) for NO (grey symbols) O₃ (black symbols) and NO₂ (open symbols) mixing ratios from profile measurements. The dotted line corresponds to a signal to noise ratio of 1.

[Title Page](#)[Abstract](#)[Introduction](#)[Conclusions](#)[References](#)[Tables](#)[Figures](#)[◀](#)[▶](#)[◀](#)[▶](#)[Back](#)[Close](#)[Full Screen / Esc](#)[Printer-friendly Version](#)[Interactive Discussion](#)

Comparison of methods for the determination of NO-O₃-NO₂ fluxes

P. Stella et al.

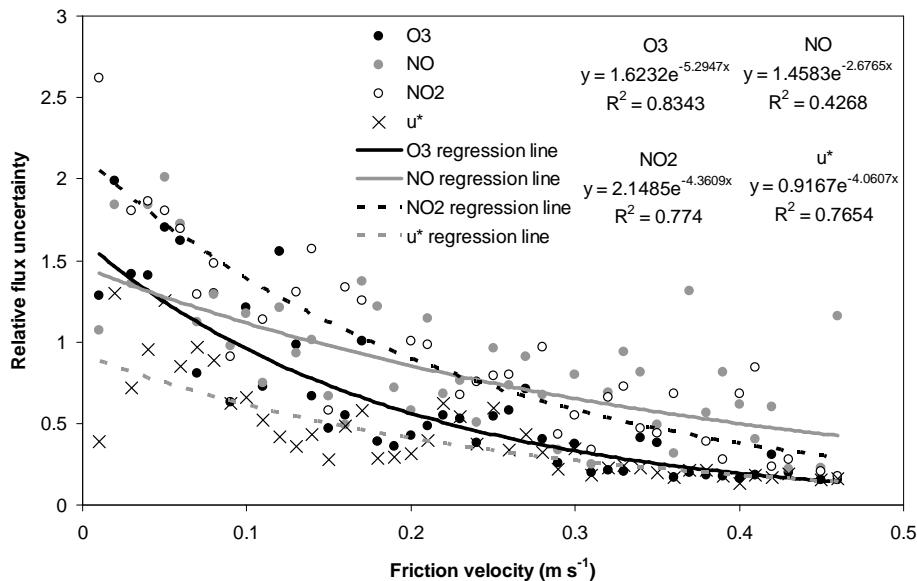


Fig. 5. Relative flux uncertainty as a function of friction velocity for O₃ (black circles), NO (grey circles), NO₂ (open circles) and u_* (crosses). Black line, grey line, black dotted line and grey dotted line are regressions for O₃, NO, NO₂ and u_* , respectively. The size of the bins used for averaging is 0.01 m s^{-1} .

[Title Page](#)
[Abstract](#)
[Introduction](#)
[Conclusions](#)
[References](#)
[Tables](#)
[Figures](#)
[⏪](#)
[⏩](#)
[◀](#)
[▶](#)
[Back](#)
[Close](#)
[Full Screen / Esc](#)
[Printer-friendly Version](#)
[Interactive Discussion](#)

Comparison of methods for the determination of NO-O₃-NO₂ fluxes

P. Stella et al.

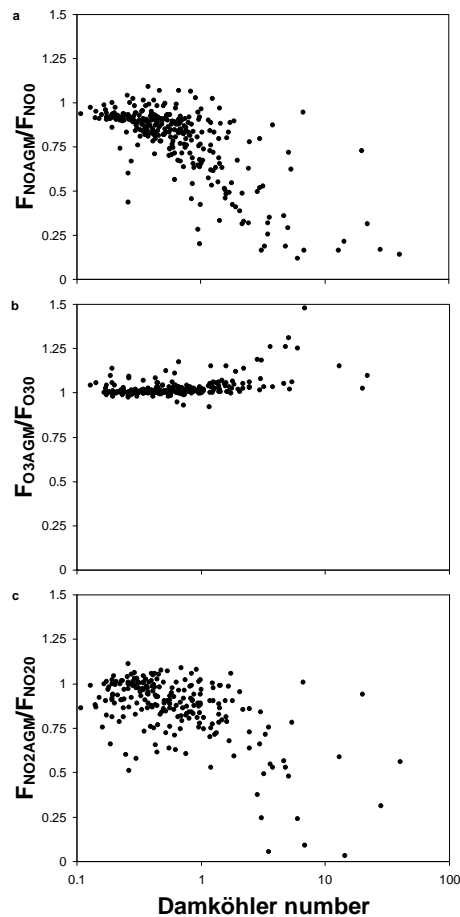


Fig. 6. Ratio of fluxes measured by AGM and surface fluxes as a function of the Damköhler number for (a) NO, (b) O₃ and (c) NO₂.

Title Page

Abstract

Introduction

Conclusions

References

Tables

Figures

◀

▶

◀

▶

Back

Close

Full Screen / Esc

Printer-friendly Version

Interactive Discussion

Comparison of methods for the determination of NO-O₃-NO₂ fluxes

P. Stella et al.

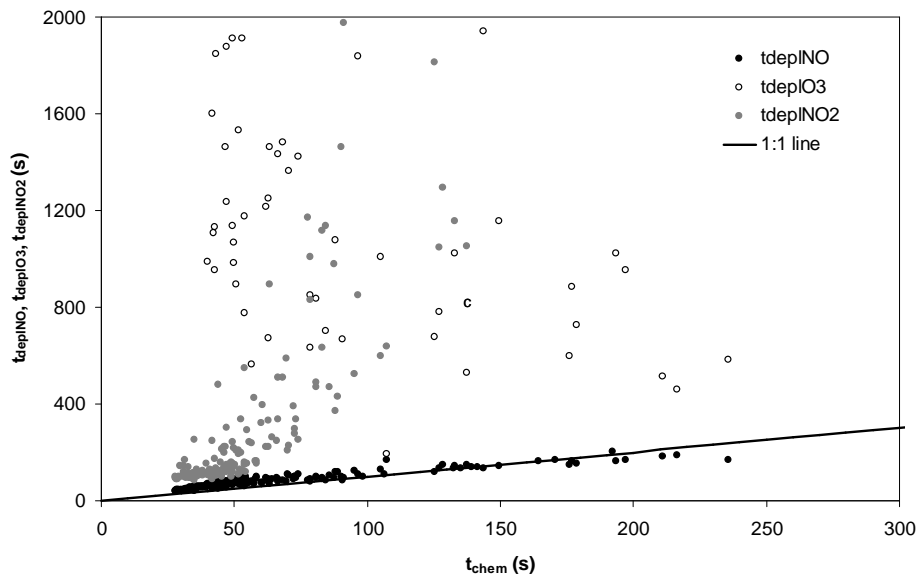


Fig. 7. Comparison between chemical reaction time for the set of chemical reactions of the NO-O₃-NO₂ triad (τ_{chem}) and chemical depletion times for NO (black symbols), O₃ (open symbols) and NO₂ (grey symbols). The black line corresponds to the 1:1 line.

[Title Page](#)[Abstract](#)[Introduction](#)[Conclusions](#)[References](#)[Tables](#)[Figures](#)[⏪](#)[⏩](#)[⏴](#)[⏵](#)[Back](#)[Close](#)[Full Screen / Esc](#)[Printer-friendly Version](#)[Interactive Discussion](#)

Comparison of methods for the determination of NO-O₃-NO₂ fluxes

P. Stella et al.

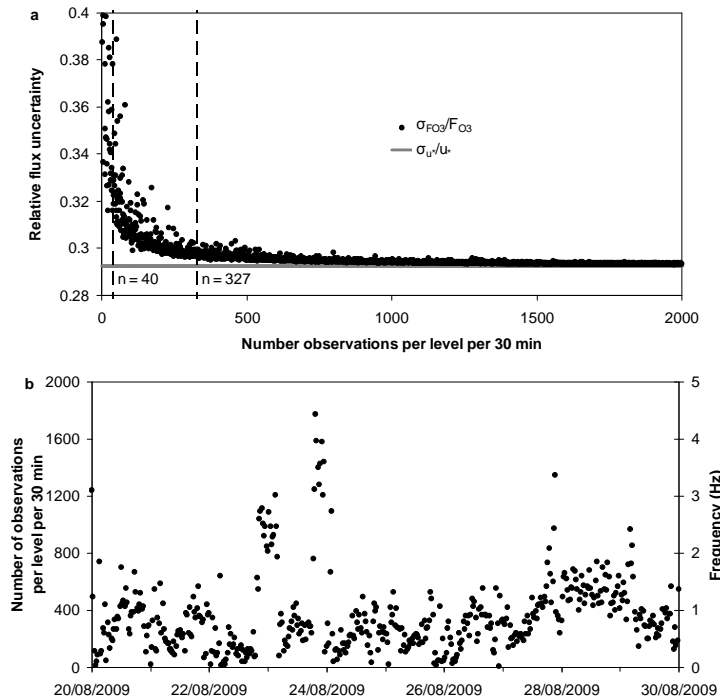


Fig. 8. (a) Relative flux uncertainty for the aerodynamic gradient method as a function of the number of concentration data available per level per 30 min. Example of the ozone flux the 25 August 2009 from 15:30 to 16:00 UT. The number of points available from measurements using the fast response sensor ($n = 327$) and under the hypothesis of the use of slow response sensor ($n = 40$) are indicated on the figure with the dashed line. (b) Time series of number of concentration points used to estimate the mean concentration at each level per 30 min based on the frequency corresponding to the inverse of the integral time scale of turbulence. This frequency corresponds to the maximum frequency above which the data are not independent and should not contribute to diminish the standard deviation as shown in (a). This frequency corresponds to the inverse of the integral time scale.

Comparison of methods for the determination of NO-O₃-NO₂ fluxes

P. Stella et al.

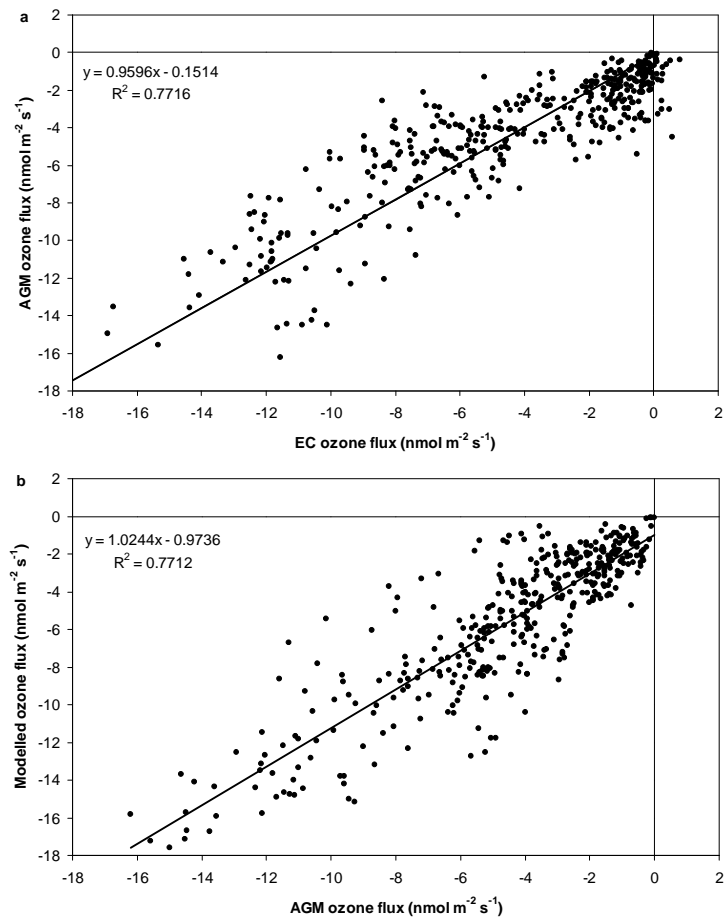


Fig. 9. Comparison between (a) ozone fluxes measured using aerodynamic gradient method and eddy-covariance method and (b) modelled and measured ozone flux. The measured fluxes were corrected for chemical reactions.

Comparison of methods for the determination of NO-O₃-NO₂ fluxes

P. Stella et al.

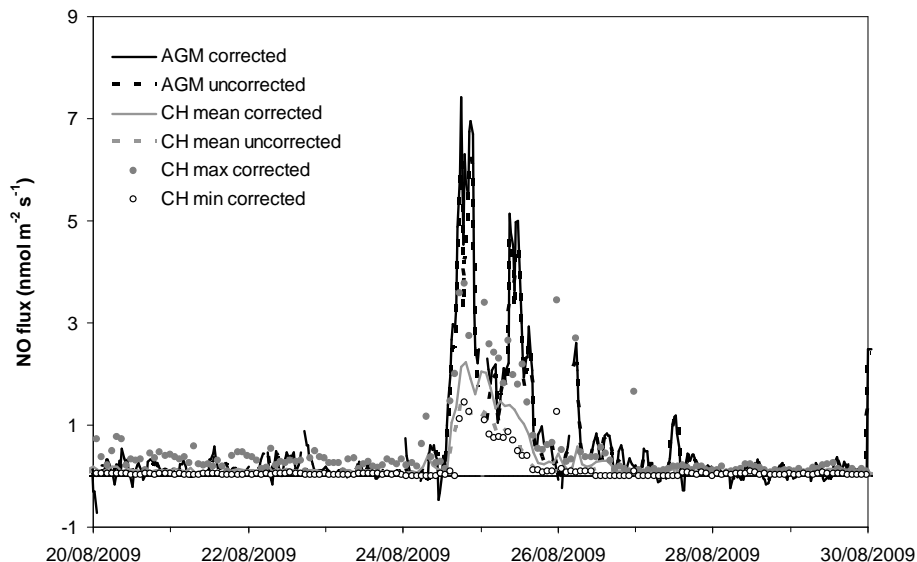


Fig. 10. Comparison between NO fluxes measured by the aerodynamic gradient method (black line) and automatic chambers (grey line). Solid and dotted lines are fluxes with and without corrections for chemical reactions, respectively. Grey and open symbols are respectively maximal and minimal NO fluxes measured by automatic chambers.

[Title Page](#)[Abstract](#)[Introduction](#)[Conclusions](#)[References](#)[Tables](#)[Figures](#)[◀](#)[▶](#)[◀](#)[▶](#)[Back](#)[Close](#)[Full Screen / Esc](#)[Printer-friendly Version](#)[Interactive Discussion](#)

Comparison of methods for the determination of NO-O₃-NO₂ fluxes

P. Stella et al.

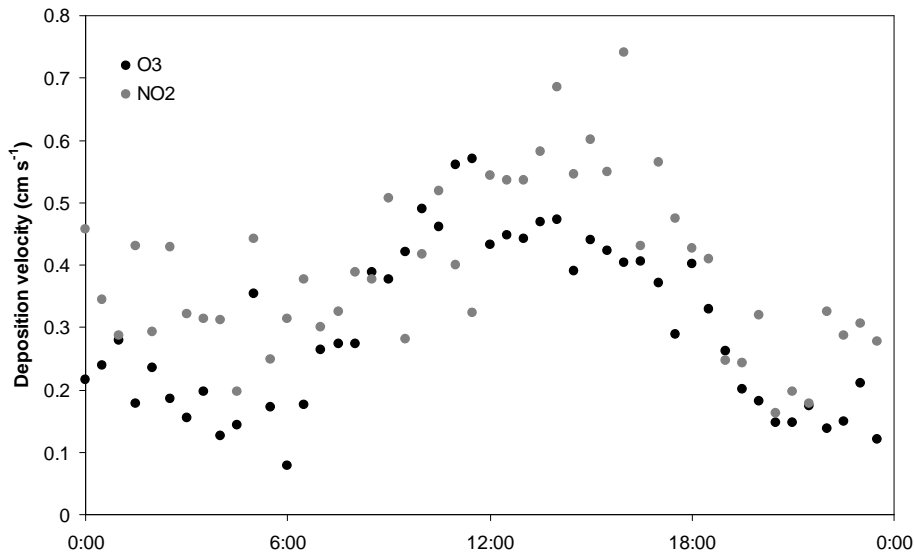


Fig. 11. Half hourly arithmetic means of ozone (black symbols) and nitrogen dioxide (grey symbols) deposition velocities at 0.61 m above the ground.

Title Page

Abstract

Introduction

Conclusions

References

Tables

Figures

◀

▶

◀

▶

Back

Close

Full Screen / Esc

Printer-friendly Version

Interactive Discussion